THE JOURNAL OF BIOLOGICAL CHEMISTRY VOL. 288, NO. 27, pp. 19739–19749, July 5, 2013

Impact of Peripheral Ketolytic Deficiency on Hepatic Ketogenesis and Gluconeogenesis during the Transition to Birth*[S]

Received for publication, January 18, 2013, and in revised form, May 15, 2013 Published, JBC Papers in Press, May 20, 2013, DOI 10.1074/jbc.M113.454868

David G. Cotter[‡§], **Baris Ercal**[‡], **D. André d'Avignon**[¶], **Dennis J. Dietzen**[§], **and Peter A. Crawford**[‡‖1]

From the [‡]*Department of Medicine, Center for Cardiovascular Research and the Departments of* [§]*Pediatrics,* [¶]*Chemistry, and* [‖]*Genetics, Washington University, St. Louis, Missouri 63110*

Background: SCOT-KO mice cannot oxidize ketone bodies and die within 48 h of birth, due to hyperketonemic hypoglycemia.
Results: After suckling milk, livers of SCOT-KO mice develop diminished pyruvate pools and alterations of hepatic pyruvate, fatty acid, and ketone body metabolism.
Conclusion: Extrahepatic ketone oxidation supports hepatic adaptation to the extrauterine environment.
Significance: Neonatal ketone metabolism reveals the importance of dynamic interorgan metabolic interactions.

Preservation of bioenergetic homeostasis during the transition from the carbohydrate-laden fetal diet to the high fat, low carbohydrate neonatal diet requires inductions of hepatic fatty acid oxidation, gluconeogenesis, and ketogenesis. Mice with loss-of-function mutation in the extrahepatic mitochondrial enzyme CoA transferase (succinyl-CoA:3-oxoacid CoA transferase, SCOT, encoded by nuclear *Oxct1*) cannot terminally oxidize ketone bodies and develop lethal hyperketonemic hypoglycemia within 48 h of birth. Here we use this model to demonstrate that loss of ketone body oxidation, an exclusively extrahepatic process, disrupts hepatic intermediary metabolic homeostasis after high fat mother's milk is ingested. Livers of SCOT-knock-out (SCOT-KO) neonates induce the expression of the genes encoding peroxisome proliferator-activated receptor γ co-activator-1a (PGC-1α), phosphoenolpyruvate carboxykinase (PEPCK), pyruvate carboxylase, and glucose-6-phosphatase, and the neonate's pools of gluconeogenic alanine and lactate are each diminished by 50%. NMR-based quantitative fate mapping of ^{13}C-labeled substrates revealed that livers of SCOT-KO newborn mice synthesize glucose from exogenously administered pyruvate. However, the contribution of exogenous pyruvate to the tricarboxylic acid cycle as acetyl-CoA is increased in SCOT-KO livers and is associated with diminished terminal oxidation of fatty acids. After mother's milk provokes hyperketonemia, livers of SCOT-KO mice diminish *de novo* hepatic β-hydroxybutyrate synthesis by 90%. Disruption of β-hydroxybutyrate production increases hepatic NAD$^+$/NADH ratios 3-fold, oxidizing redox potential in liver but not skeletal muscle. Together, these results indicate that peripheral ketone body oxidation prevents hypoglycemia and supports hepatic metabolic homeostasis, which is critical for the maintenance of glycemia during the adaptation to birth.

At birth, a transplacental nutrient stream replete with carbohydrates is terminated and replaced with a high fat, low carbohydrate milk diet that is cyclically interrupted by periods of nutrient deprivation. Hepatic glucose production plays a critical role in providing fuel, particularly to the developing brain (1). Nonetheless, glucose utilization is thought to support only ~70% of the neonatal brain's energetic needs, and additional substrates, including ketone bodies, are required to supply the balance (2). To meet this demand, a coordinated hepatic metabolic program integrates β-oxidation and terminal oxidation of fatty acids, gluconeogenesis, and ketogenesis (1). Ketone body metabolism mediates energy transfer by partially oxidizing hepatic fatty acids to water-soluble four-carbon ketone body intermediates that are transported to extrahepatic organs for terminal oxidation during physiological states characterized by limited carbohydrate supply (3–5). As such, contributions of ketone body metabolism to neonatal bioenergetic homeostasis are 2-fold: (i) because the neonatal diet has high lipid content, ketogenesis provides a spillover pathway for excess fatty acid oxidation-derived acetyl-CoA that would otherwise require terminal oxidation, storage, or secretion (4, 6, 7); and (ii) extrahepatic ketone body oxidation diminishes hepatic gluconeogenic demand because ketone body oxidation spares glucose utilization in peripheral tissues (3).

Most ketogenesis occurs within hepatic mitochondria, at rates proportional to β-oxidation of fatty acids (4). Sequential ketogenic reactions catalyzed by mitochondrial thiolase, mitochondrial hydroxymethylglutaryl-CoA synthase (HMGCS2),[2] and hydroxymethylglutaryl-CoA lyase convert β-oxidation-de-

* This work was supported by National Institutes of Health Grant DK091538 (to P. A. C.) and Training Grant HL007873 (to D. G. C.). This work was also supported by the March of Dimes and the Children's Discovery Institute through St. Louis Children's Hospital (to P. A. C.).
[S] This article contains supplemental Figs. S1–S6 and Tables S1–S7.
[1] To whom correspondence should be addressed: Dept. of Medicine, Division of Cardiology, Washington University School of Medicine, Campus Box 8086, 660 S. Euclid Ave., St. Louis, MO 63110. Tel.: 314-747-3009; Fax: 314-219-4589; E-mail: pcrawford@wustl.edu.

[2] The abbreviations used are: HMGCS2, mitochondrial hydroxymethylglutaryl-CoA synthase; AcAc, acetoacetate; BDH1, D-βOHB-dehydrogenase; D-βOHB, D-β-hydroxybutyrate; gHSQC, gradient heteronuclear single-quantum correlation; MS/MS, tandem MS; PDH, pyruvate dehydrogenase; P*n*, postnatal day *n*; SCOT, succinyl-CoA:3-oxoacid CoA transferase; TCA, tricarboxylic acid.

rived acetyl-CoA to the ketone body acetoacetate (AcAc), which is reduced by mitochondrial D-β-hydroxybutyrate (D-βOHB)-dehydrogenase (BDH1) to D-βOHB in an NAD^+/NADH-coupled redox reaction (8–10). Within extrahepatic organs, mitochondrial BDH1 reoxidizes D-βOHB to AcAc. Covalent activation of AcAc by CoA is catalyzed by the mitochondrial matrix enzyme succinyl-CoA:3-oxoacid CoA transferase (SCOT (encoded by the nuclear gene *Oxct1*), the only mammalian CoA transferase) to generate AcAc-CoA, which upon thiolytic cleavage, liberates acetyl-CoA that enters the tricarboxylic acid (TCA) cycle for terminal oxidation (11). CoA transferase catalyzes a near equilibrium reaction in which coenzyme A is exchanged between succinate and AcAc (12). Ketone bodies are efficient energetic substrates that are oxidized in proportion to their delivery (1, 3, 4). The neonatal brain extracts ketones at rates up to 40-fold greater than the adult brain, and ketone body oxidation can support as much as 25% of the neonate's total basal energy requirements (2, 13). Because neurons oxidize fatty acids poorly (2, 14), ketogenesis has been proposed as a key determinant in vertebrate evolution and the evolution of human brain size (15).

Prior analysis of germline CoA transferase knock-out (SCOT-KO) mice revealed that CoA transferase is required for terminal ketone body oxidation. SCOT-KO mice are born normal, but exhibit increased cerebral glucose oxidation. These mice ultimately develop hyperketonemic hypoglycemia and die within 48 h of birth unless their lifespan is prolonged by frequent glucose administration (16). Unlike mice with a global CoA transferase defect, recent studies using cell type-specific SCOT-KO mice reveal that the selective absence of ketone body oxidation individually within neurons, cardiomyocytes, or skeletal myocytes (the three greatest consumers of ketone bodies (3, 17)) does not cause hyperketonemia or hypoglycemia and does not impair survival during the neonatal period or starvation in adulthood. As observed in brains of germline SCOT-KO neonates, selective absence of neuronal CoA transferase activity was associated with increased glycolysis and glucose oxidation in the neonatal brain (18). Taken together, the phenotypes of germline and tissue-specific SCOT-KO mice reveal that ketolytic cells do not require the energy stored in ketone bodies, but ketone body oxidation is necessary for maintenance of glycemia and therefore survival in the neonatal period.

During states in which dietary carbohydrates are in short supply, the balance of hepatic glucose output with extrahepatic glucose consumption coordinates glucose homeostasis. Increased extrahepatic glucose consumption in neonatal germline SCOT-KO mice may therefore contribute to the development of hypoglycemia. To determine whether the absence of extrahepatic ketone body oxidation influences hepatic glucose production and intermediary metabolic homeostasis, we used biochemical approaches to quantify dynamic metabolism in livers of germline neonatal SCOT-KO mice.

EXPERIMENTAL PROCEDURES

Animals—Oxct1$^{-/-}$ (germline SCOT-KO) mice were generated on the C57BL/6 genetic background (16). To obtain unfed neonatal mice, pups were collected within 1 h of birth. Pups without gastric milk spots were confirmed by open examination of the stomach and intestine at the time of sacrifice. Fed postnatal day zero (P0, the first day of postnatal life) mice were collected within 4 h of birth. All postnatal day 1 (P1) mice were maintained with the dam through the first 30 h after birth and were milk-fed. All mice were maintained at 22 °C on standard polysaccharide-rich chow diet (Lab Diet 5053) and autoclaved water *ad libitum*. Lights were off between 1800 and 0600. All experiments consisted of mouse pups that were harvested from at least three litters from three different breeder pairings. All experiments were conducted using protocols approved by the Animal Studies Committee at Washington University.

Plasma Metabolite Measurements—Measurements of plasma AcAc and D-βOHB were performed using standard biochemical assays coupled to colorimetric substrates (Wako), as described previously (19). AcAc concentrations were determined by measuring total ketone body concentrations and subtracting the corresponding measured D-βOHB concentration. Plasma lactate and pyruvate were measured using colorimetric and fluorescent biochemical assays, respectively (Biovision). Blood glucose was measured in duplicate using glucometers (Aviva).

Gene Expression Analysis—Quantification of gene expression was performed using real-time RT-quantitative PCR using the ΔΔCt approach as described, normalizing to *Rpl32*, using primer sequences listed within supplemental Table S1 (19).

Immunoblotting—Immunoblotting, using protein lysates from neonatal brain, heart, liver, and quadriceps/hamstring muscles to detect SCOT (rabbit anti-SCOT; Proteintech Group), actin (rabbit anti-actin; Sigma), HMGCS2 (rabbit anti-mHMGCS; Santa Cruz Biotechnology), PDH-E1α (rabbit anti-pyruvate dehydrogenase E1-α subunit antibody; Abcam ab155096), phosphoserine 293 PDH-E1α (PhosphoDetect™ anti-PDH-E1α (Ser(P)-293 rabbit antibody; Millipore AP1062), and BDH1 (rabbit anti-BDH1; Proteintech Group) was performed as described previously (34). Band intensities were quantified densitometrically using QuantityOne software (Bio-Rad).

In Vitro Ketogenesis of Hepatic Explants—Neonatal mice were sacrificed by decapitation. Livers were collected and weighed, and each liver was placed in a single well of a 6-well tissue culture plate containing 2 ml of phosphate-buffered saline (PBS) on ice. Livers were minced and transferred to a 2-ml Eppendorf tube. Tissues were allowed to settle on ice and were centrifuged at 500 × *g* for 1 min. Minced-liver pellets were resuspended in 1 ml of assay medium (Dulbecco's modified Eagle's medium supplemented with 2.78 mM glucose (which reflects glycemia in neonatal mice), 0.63 mM sodium pyruvate, and 150 μM oleic acid (conjugated to bovine serum albumin in a 2:1 molar ratio)). Each liver preparation was plated in a single well of a 12-well plate containing 1 ml of medium, and incubated at 37 °C. At time points indicated in the figure legends, 50 μl of medium was removed to quantify ketone body concentrations.

Tissue Triglyceride, Glycogen, and Nicotinamide Metabolite Quantifications—Hepatic triacylglycerol concentrations were determined using a Folch extract of liver and biochemical quantification using a biochemical assay (Wako), as described previously (20). Hepatic glycogen and NAD^+(H) concentrations

were measured in liver lysates using fluorescent biochemical assays (Biovision).

In Vivo Substrate Utilization—P0 or P1 mice were injected intraperitoneally with 10 μmol of sodium [1,2,3,4-$^{13}C_4$]octanoate, 10 μmol of sodium [3-^{13}C]pyruvate, or co-injected with 10 μmol of sodium [1,2,3,4-$^{13}C_4$]octanoate, plus 20 μmol of naturally occurring sodium pyruvate, sodium D-βOHB, sodium L-βOHB, or AcAc per g of body weight (vendor for stable isotopes: Cambridge Isotope Laboratories). Base hydrolysis of ethyl-AcAc (Sigma W241512) was performed by addition of 50% NaOH to pH 12 and incubation at 60 °C for 30 min. The pH of base-hydrolyzed AcAc was adjusted to pH 8.5, and [AcAc] was confirmed using standard biochemical assays coupled to colorimetric substrates (Wako), as described previously (19). After intraperitoneal injections, neonatal mice were maintained on a heating pad for the indicated durations (see text and figure legends), killed by decapitation, and tissues were rapidly freeze-clamped in liquid N_2. Neutralized perchloric acid tissue extracts were profiled using ^{13}C-edited proton nuclear magnetic resonance (NMR) measured at 11.75 Tesla (Varian/Agilent Direct Drive-1) via first increment gradient heteronuclear single-quantum correlation (gHSQC). The majority of studies were carried out using a traditional probe, but extracts generated from mice injected with sodium [3-^{13}C]pyruvate were analyzed using a high sensitivity cold probe at 11.75 Tesla (Varian/Agilent Direct Drive-1). Signals were collected from extracts dissolved in 275 μl of D_2O + 1 mM trimethylsilyl propionate, loaded into high precision, thin walled 5-mm tubes (Shigemi). Quantification of signals by integration from the ^{1}H{^{13}C} and ^{13}C-edited (gHSQC) collections of carbon 2 for taurine, carbon 4 for βOHB, carbon 1 for glucose, carbon 4 for glutamate, and ^{1}H{^{13}C} of carbon 3 for lactate were all performed as described previously (16). Tissue concentrations (pool size) of glucose, taurine, glutamate, and βOHB were calculated by normalizing the integrals for each metabolite obtained from the ^{1}H{^{13}C} collections to trimethylsilyl propionate and tissue weight. Because tissue taurine concentrations were constant across conditions (supplemental Tables S2 and S3) and taurine is not enriched by administration of these experimental substrates (19, 21), taurine was used as a normalizing metabolite between the ^{1}H{^{13}C} and gHSQC collections to calculate the moles of ^{13}C-labeled metabolites present in each sample. The moles of ^{13}C-labeled metabolites produced from the labeled substrate in each sample were calculated by subtracting the moles of ^{13}C-labeled metabolites attributable to the metabolite pool size (*i.e.* in the absence of any enrichment from exogenous ^{13}C-labeled substrates, 1.1% of the metabolites within the entire pool are expected to be ^{13}C-labeled, based upon the natural abundance of ^{13}C) from the total amount of ^{13}C-labeled metabolites detected in the gHSQC collections. Fractional enrichments of ^{13}C-labeled glutamate and βOHB were then calculated as described (19) by dividing taurine-normalized integral values for each queried metabolite derived from the gHSQC collections by the corresponding integral value obtained from the ^{1}H{^{13}C} collections.

Tandem Mass Spectrometry (MS/MS) Analysis of Blood Amino Acids and Acylcarnitines—Neonatal blood was spotted onto 1.3-cm spots on Whatman 903 filter paper. Amino acids were quantified as butyl ester derivatives using multiple precursor/product combinations in a reversed-phase liquid chromatography protocol coupled to MS/MS (22). Carnitine esters were measured by scanning for the precursors of the common *m*/*z* 85 carnitine fragment. Quantification was achieved in all cases using stable isotope ^{2}H-labeled internal standards using an electrospray ionization source coupled to an API 3200-Qtrap tandem mass spectrometer (Applied Biosystems).

RESULTS

Neonatal SCOT-KO Mice Engage a Hepatic Gluconeogenic Gene Program—The liver is the most important source of glucose for the neonatal brain (2, 23), which increases its reliance on this vital fuel when CoA transferase inactivation prevents ketone body oxidation in the entire brain (16) or selectively within neurons (18). Therefore, we hypothesized that neonatal germline SCOT-KO mice, which cannot terminally oxidize ketone bodies, engage compensatory mechanisms in the liver to meet increased peripheral glucose demand. Increased abundances of the mRNAs encoding peroxisome proliferator-activated receptor γ co-activator-1a (PGC-1α, encoded by *Ppargc1a*), pyruvate carboxylase (encoded by *Pcx*), phosphoenolpyruvate carboxykinase (PEPCK, encoded by *Pck1*), and glucose-6-phosphatase (encoded by *G6pc*) were observed in livers of postnatal day 1 (P1, the day immediately following delivery) SCOT-KO mice (Fig. 1*A*), and as expected, hepatic glycogen content was depleted in livers of P1 SCOT-KO mice (Fig. 1*B*). Consistent with increased gluconeogenic demand, MS/MS analysis of circulating amino acids demonstrated that alanine, which becomes the gluconeogenic substrate pyruvate following transamination (24), was diminished 51% in blood of P1 SCOT-KO mice (Fig. 1*C*). Serine, which is deaminated to pyruvate by serine dehydratase, also trended lower in these mice. In addition, blood concentrations of the anaplerotic amino acid glutamate, which can replenish TCA cycle intermediates following conversion to α-ketoglutarate, were diminished 40% in SCOT-KO neonates. This contrasted with many glucogenic/ketogenic, glucogenic, ketogenic, and urea cycle amino acids, whose circulating concentrations were increased in P1 SCOT-KO mice (Fig. 1*D*; see supplemental Tables S4 and S5 for complete P0 and P1 blood amino acid profiles, respectively, of wild-type and SCOT-KO mice), suggesting enhanced skeletal muscle proteolysis in P1 SCOT-KO mice. In addition, the total circulating pyruvate pool (the sum of pyruvate plus lactate, which form a redox couple with NAD^+/NADH), a critical source of gluconeogenic precursors via the Cori cycle, was diminished 53% in P1 SCOT-KO mice (Fig. 1*E*). In SCOT-KO neonates, increased extrahepatic glucose and lactate consumption (16, 18) are likely contributors to hypoglycemia. Unlike wild-type littermates, endogenous hepatic content of free glucose was below the limit of detection by proton NMR in P1 SCOT-KO mice (Fig. 1*F*, *left*), suggesting that hepatic glucose generated from residual endogenous substrates is rapidly cleared to meet increased peripheral demands and that this production is insufficient to support the glycemic requirements for survival in these mice. However, intraperitoneal supplementation of P1 SCOT-KO mice with exogenous [^{13}C]pyruvate 30 min prior to harvest of the liver demonstrated robust gener-

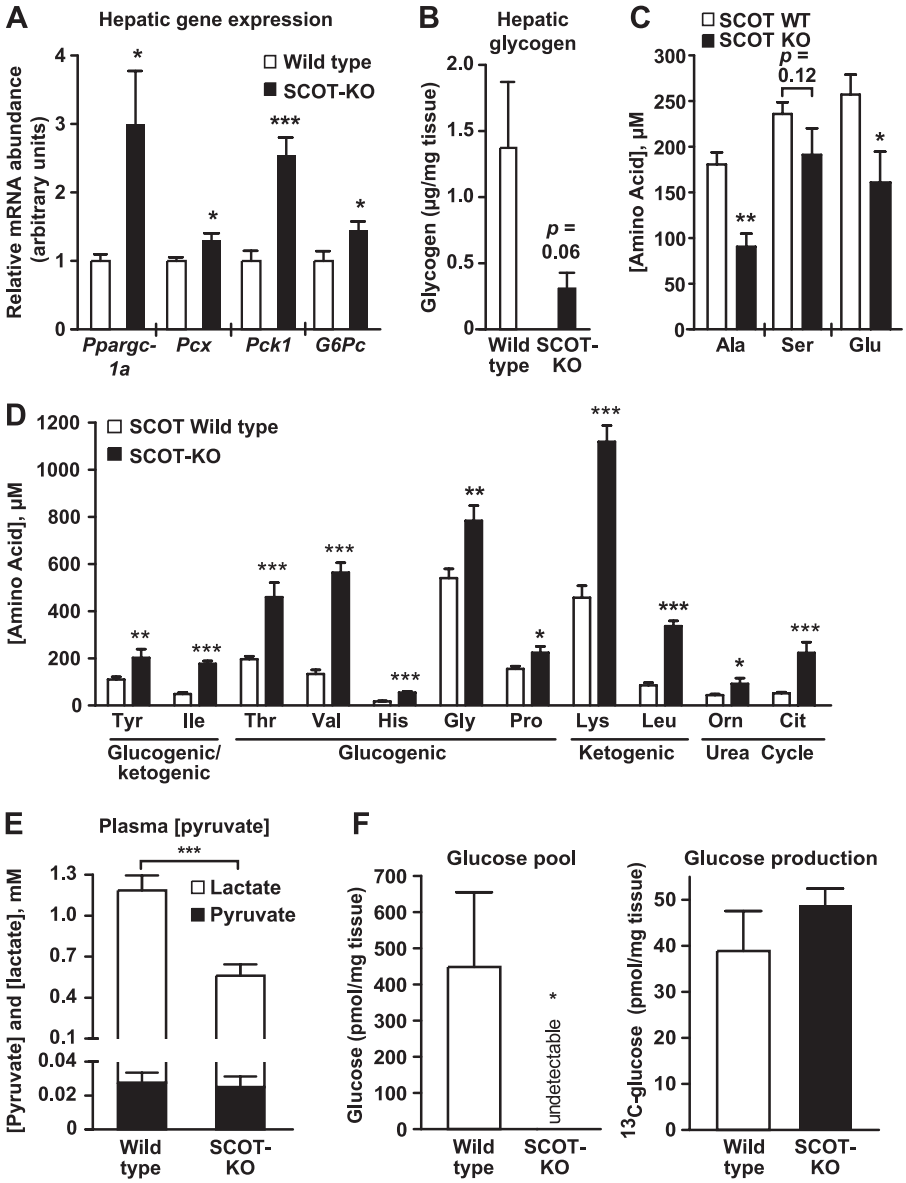

FIGURE 1. **Absence of extrahepatic ketone body oxidation engages an hepatic gluconeogenic program in neonatal mice.** *A*, relative mRNA abundance of encoded mediators of pyruvate metabolism and gluconeogenesis in livers of P1 mice. $n = 5$/group. *B*, liver glycogen content (μg of glycogen/mg of tissue) in P1 neonates. $n = 8$/group. $p = 0.06$ by Student's *t* test. *C*, blood alanine, serine, and glutamate concentrations (micromolar) in P1 mice. $n = 5$–7/group. *D*, circulating amino acid concentrations (micromolar) in blood of P1 mice. $n = 5$–10/group. *E*, plasma pyruvate pool (pyruvate + lactate) in P1 mice. $n = 8$–11/group. *F*, endogenous hepatic glucose concentration (*left*) and accumulated [^{13}C]glucose in livers (*right*) of P1 mice that had been injected with [3-^{13}C]pyruvate (10 μmol/g of body weight) 30 min prior to collection of tissues and generation of extracts for NMR. $n = 4$/group. *, $p < 0.05$; **, $p < 0.01$; ***, $p < 0.001$ by Student's *t* test. *Error bars*, S.E.

ation of [^{13}C]glucose (Fig. 1*F*, *right*). Taken together, these data suggest that neonatal hepatic glucose production is increased to meet enhanced peripheral requirements, but is limited in these mice by precursor availability and not intrinsic synthetic capacity.

Reprogrammed Intermediary Metabolism in Livers of Neonatal SCOT-KO Mice—Given marked hypoglycemia, hyperketonemia, alterations of gluconeogenic precursor pools, and increased concentrations of circulating amino acids, we hypothesized that livers of P1 SCOT-KO mice would exhibit alterations of terminal fatty acid oxidation and pyruvate metabolism. Therefore, to determine whether livers of P1 germline SCOT-KO mice exhibit diminished terminal oxidation of acyl-CoA-derived acetyl-CoA, we quantified the contribution of the fatty acid [1,2,3,4-$^{13}C_4$]octanoate (10 μmol/g body weight, via the intraperitoneal route) to the acetyl-CoA entering the TCA cycle, by using [^{13}C]glutamate fractional enrichment as a quantitative surrogate because glutamate is in equilibrium with the TCA cycle intermediate α-ketoglutarate (16, 18, 19, 21, 25, 26). Hepatic enrichment of [^{13}C]glutamate did not differ between P1 wild-type and SCOT-KO mice that received [^{13}C]octanoate alone (Fig. 2*A*, *left*), indicating equal contributions of labeled octanoate to the acetyl-CoA entering the TCA cycle. However, SCOT-KO mice exhibited a significantly decreased glutamate pool size (Fig. 2*A*, *right*; 1.03 ± 0.17 nmol of glutamate/mg liver in P0 wild-type mice *versus* 0.56 ± 0.09 nmol of glutamate/mg liver in P1 SCOT-KO mice, $p = 0.046$, $n = 6-8$/group). Therefore, to determine whether hepatic terminal fatty acid oxidation

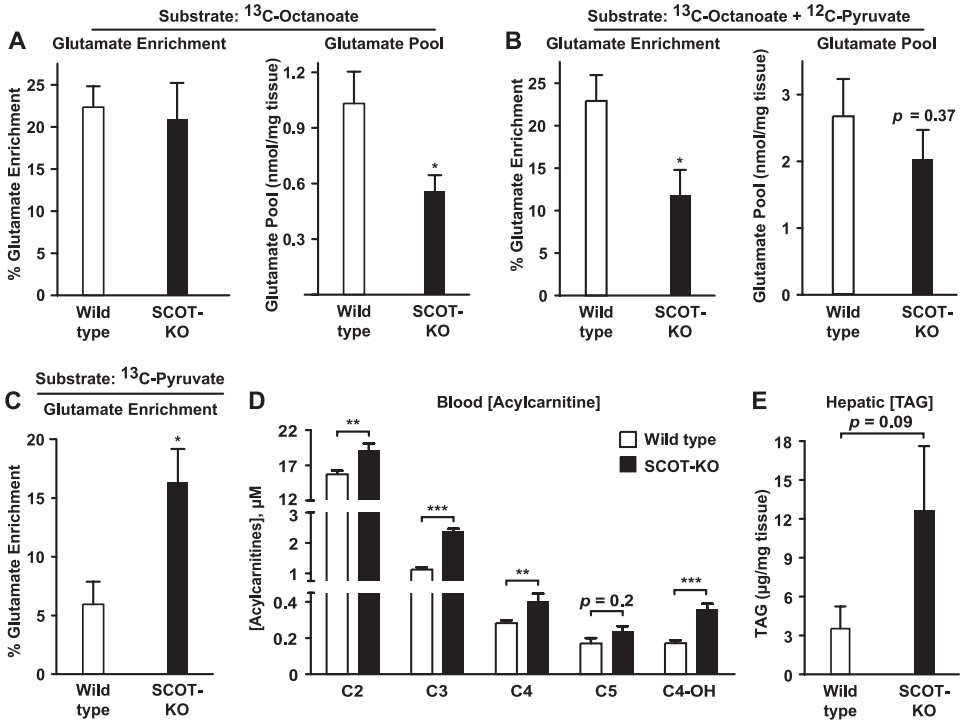

FIGURE 2. **Alterations of terminal fatty acid oxidation and pyruvate handling in livers of SCOT-KO mice.** *A*, hepatic fractional ^{13}C enrichments of glutamate (*left*) and total hepatic glutamate pools (*right*) 20 min after intraperitoneal injection of sodium [1,2,3,4-$^{13}C_4$]octanoate (10 μmol/g of body weight) in P1 mice. $n = 6–8$/group. *B*, fractional ^{13}C enrichments of glutamate (*left*) and total hepatic glutamate pools (*right*) 20 min after intraperitoneal injection of sodium [1,2,3,4-$^{13}C_4$]octanoate (10 μmol/g of body weight) + unlabeled pyruvate (20 μmol/g) in livers P1 mice. $n = 6–7$/group. *C*, fractional ^{13}C enrichments of glutamate 30 min after intraperitoneal injection of sodium [3-^{13}C]pyruvate (10 μmol/g of body weight) in livers of P1 mice. $n = 4$/group. *D*, short chain acylcarnitine concentrations in blood of untreated P1 mice. $n = 5–10$/group. *E*, hepatic triacylglycerol (TAG) content in livers of untreated P1 mice. $n = 5–6$/group. *, $p < 0.05$; **, $p < 0.01$; ***, $p < 0.001$ by Student's *t* test. *Error bars*, S.E.

remains equal when glutamate pool sizes in livers of P1 wild-type and SCOT-KO mice are equal, we co-administered [^{13}C]octanoate with unlabeled pyruvate, which augments TCA cycle intermediates by stimulating anaplerosis. Co-administration of unlabeled pyruvate with [^{13}C]octanoate increased hepatic glutamate pool sizes in livers of both wild-type and SCOT-KO neonatal mice and abrogated the diminution of this pool size in livers of SCOT-KO mice (Fig. 2*B*, *right*). However, compared with livers of wild-type P1 mice, hepatic glutamate enrichment from [^{13}C]octanoate was diminished nearly 50% in livers of P1 SCOT-KO mice delivered this combination of substrates (22.9 ± 3.05% in wild-type mice *versus* 11.8 ± 3.0% in SCOT-KO mice, $p = 0.026$, $n = 6–7$/group; Fig. 2*B*, *left*), indicating diminished contribution of labeled octanoate to the acetyl-CoA entering the TCA cycle in livers of P1 SCOT-KO mice. The only competing sources of acetyl-CoA in the livers of neonatal mice in this experimental context are (i) endogenous fatty acids or (ii) pyruvate that is decarboxylated via the PDH complex. Thus, we directly quantified the contribution of pyruvate to the acetyl-CoA entering the TCA cycle by administering [3-^{13}C]pyruvate (10 μmol/g of body weight), which labels >95% of the circulating pyruvate pool in both wild-type and SCOT-KO mice and measured hepatic glutamate enrichment. Hepatic ^{13}C enrichment of glutamate was 2.7-fold greater in SCOT-KO neonates administered [^{13}C]pyruvate (5.95 ± 1.92% *versus* 16.32 ± 2.87% in livers of wild-type and SCOT-KO P1 mice, respectively, $p = 0.04$, $n = 4$/group; Fig. 2*C*). As observed in mice receiving unlabeled pyruvate (Fig. 2*B*), hepatic glutamate pools were not different between wild-type and SCOT-KO neonates injected with [^{13}C]pyruvate (data not shown). Increased [^{13}C]glutamate enrichment from [^{13}C]pyruvate occurred in SCOT-KO neonates in the absence of altered phosphorylation of PDH on the E1 α subunit, a post-translational modification that increases the K_m of PDH (27–29) (supplemental Fig. S1).

Because the contribution of labeled fatty acids to the acetyl-CoA entering the TCA cycle was diminished in livers of P1 SCOT-KO mice when glutamate pools were rendered equal by administration of unlabeled pyruvate, we hypothesized that signatures of diminished fatty acid oxidation would be evident in livers of these mice. To determine whether there was a defect in the β-oxidation spiral, we quantified blood acylcarnitines of untreated P1 germline SCOT-KO mice by MS/MS. Whereas medium and long chain acylcarnitine species were normal (supplemental Table S6), short chain acylcarnitine concentrations were elevated in P1 SCOT-KO mice (Fig. 2*D*). This result is consistent with an intact β-spiral, but diminished entry of its products into the TCA cycle. Abundances of transcripts encoding key mediators of fatty acid transport and oxidation, including *Fabp1*, *Fgf21*, *Cpt1a*, and *Acadm* mRNAs, were all normal in SCOT-KO mice (supplemental Fig. S2*A*). However, hepatic triacylglycerol content trended higher in P1 SCOT-KO mice (Fig. 2*E*; 12.7 ± 5.0 μg/mg of liver *versus* 3.5 ± 1.7, respectively, $p = 0.09$, $n = 5–6$/group), also suggesting impaired terminal fatty acid oxidation in livers of SCOT-KO mice.

To determine whether signatures of diminished terminal fatty acid oxidation in livers of SCOT-KO neonatal mice are innate or the result of a perturbed metabolic environment, we delivered [^{13}C]octanoate to newborn P0 SCOT-KO mice that had been collected prior to their first milk feed and observed that hepatic [^{13}C]glutamate fractional enrichment and glutamate pool size were both normal, as they were in livers of fed P0 SCOT-KO mice (supplemental Fig. S3). Moreover, unlike the observation of increased short chain acylcarnitines in the circulation of P1 SCOT-KO mice, blood acylcarnitine species did not differ between fed, but untreated P0 wild-type and SCOT-KO mice (supplemental Table S7). Taken together, these findings indicate that the observed abnormalities of fatty acid and pyruvate metabolism are likely secondary to increased gluconeogenic demand and the hyperketonemic state that develops in P1 SCOT-KO mice.

Accumulated D-βOHB Suppresses Normal Ketogenesis in Neonatal Liver—Due to (i) the alterations of hepatic fatty acid oxidation and pyruvate metabolism in SCOT-KO mice and (ii) our previous observation that the AcAc/βOHB ratio was significantly elevated in the circulation of markedly hyperketonemic P1 SCOT-KO mice (16), we hypothesized that regulation of hepatic ketogenesis would also be altered in these mice. To determine the effects of peripheral ketolytic deficiency on hepatic ketogenesis, we measured the hepatic ^{13}C fractional enrichment and pool sizes of βOHB in neonatal mice injected with [^{13}C]octanoate. ^{13}C-βOHB enrichment from [^{13}C]octanoate was decreased 15-fold in livers of P1 SCOT-KO mice (15.26 ± 1.34% *versus* 1.21 ± 0.08%, $p < 0.0001$, $n = 6-8$/group, Fig. 3*A*, *left*). Commensurate with the marked increase in the concentration of circulating ketone bodies in P1 SCOT-KO mice, the total hepatic βOHB pool size was expanded in P1 SCOT-KO mice (0.51 ± 0.07 nmol of βOHB/mg of liver and 3.27 ± 0.73 nmol of βOHB/mg of liver in wild-type and SCOT-KO mice, respectively, $p = 0.0009$, $n = 6-8$/group; Fig. 3*A*, *middle*). Therefore, to confirm that the decreased ^{13}C-βOHB fractional enrichment from [^{13}C]octanoate in livers of SCOT-KO mice reflects diminished *de novo* production of βOHB (rather than merely an increase in the total pool), we quantified the ^{13}C-βOHB abundance in livers of these mice and observed a 90% decrease in livers of P1 SCOT-KO mice (72.4 ± 12.5 pmol of ^{13}C-βOHB/mg of liver and 6.3 ± 2.1 pmol of ^{13}C-βOHB produced/mg of liver in wild-type and SCOT-KO mice, respectively, $p = 0.0007$, $n = 6-8$/group; Fig. 3*A*, *right*). Messenger mRNAs encoding the ketogenic mediators FGF21 and HMGCS2 were both normal, whereas *Bdh1* mRNA abundance was decreased 50% in livers of P1 SCOT-KO mice (supplemental Fig. S2*A*). At the protein level, SCOT-KO livers exhibited ~25% increased HMGCS2 and normal BDH1 protein abundance (supplemental Fig. S2, *B* and *C*).

To determine whether the marked impairment of βOHB production in livers of P1 SCOT-KO mice was innate or acquired, we quantified ^{13}C-βOHB production from [^{13}C]-octanoate in livers of unfed P0 SCOT-KO mice. Hepatic ^{13}C-βOHB enrichment, βOHB pool size, and ^{13}C-βOHB production were all normal in unfed P0 SCOT-KO mice (Fig. 3*B*). Prior to milk feeding, endogenous plasma ketones were nearly undetectable and did not differ between wild-type and SCOT-KO mice (Fig. 3*C*). However, after only a single feed, plasma ketone bodies exceeded 3 mM in SCOT-KO mice (*versus* ~0.3 mM in wild-type littermate controls), with both D-βOHB and AcAc exhibiting significant increases in SCOT-KO neonates (Fig. 3*D*). In contrast to the robust ^{13}C labeling of hepatic βOHB in

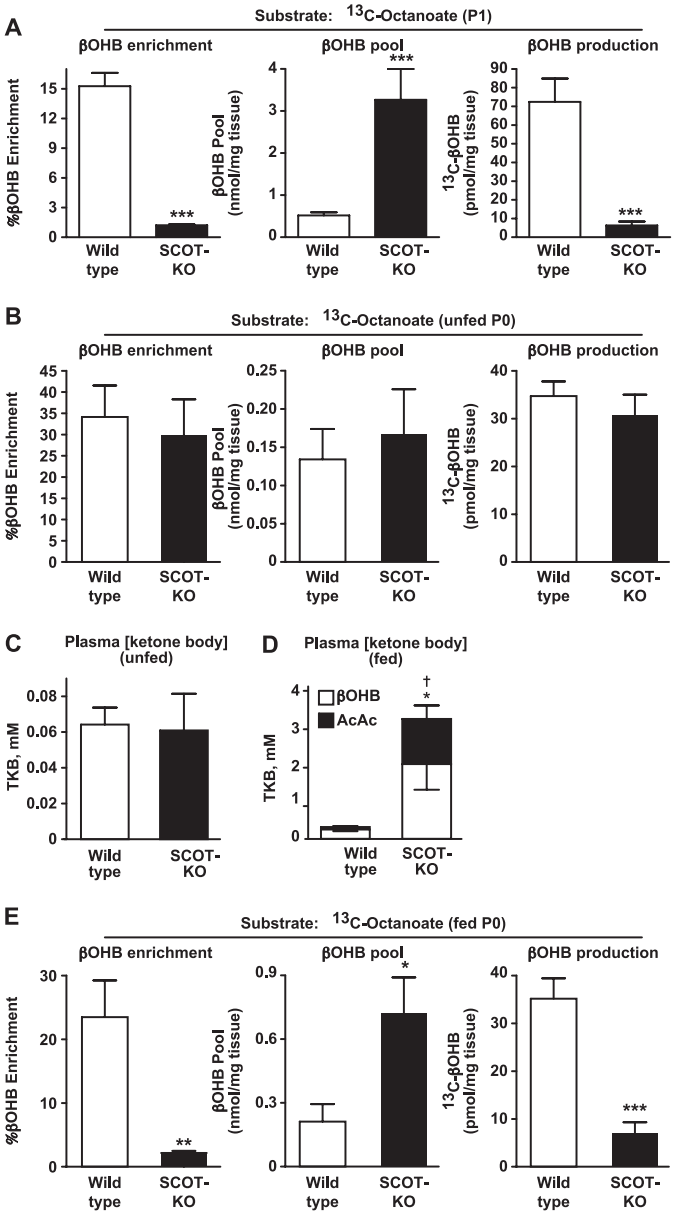

FIGURE 3. **Mother's milk-induced impairment of *de novo* βOHB production in neonatal SCOT-KO liver.** *A*, hepatic fractional ^{13}C enrichments of βOHB (*left*), total βOHB pools (*middle*), and ^{13}C-βOHB concentration (*right*) 20 min after intraperitoneal injection of sodium [1,2,3,4-$^{13}C_4$]octanoate (10 μmol/g of body weight) in P1 mice. $n = 6-8$/group. *B*, fractional ^{13}C enrichments of βOHB (*left*), total βOHB pools (*middle*), and ^{13}C-βOHB concentration (*right*) 20 min after intraperitoneal injection of sodium [1,2,3,4-$^{13}C_4$]octanoate (10 μmol/g of body weight) in livers of unfed P0 mice. $n = 6$/group. *C*, plasma total ketone body (TKB) concentration (millimolar), measured in P0 wild-type and SCOT-KO mice prior to the onset of suckling. $n = 4$/group. *D*, plasma total ketone body concentration (millimolar), measured in P0 wild-type and SCOT-KO mice within 2 h after the onset of suckling. The distributions of D-βOHB and AcAc are shown. $n = 8-10$/group. †, $p < 0.05$ for AcAc; *, $p < 0.05$ for βOHB. *E*, fractional ^{13}C enrichments of βOHB (*left*), total βOHB pools (*middle*), and ^{13}C-βOHB concentration (*right*) 20 min after intraperitoneal injection of sodium [1,2,3,4-$^{13}C_4$]octanoate (10 μmol/g of body weight) in milk-fed P0 mice. $n = 6-7$/group. ***, $p < 0.001$ by Student's *t* test. *Error bars*, S.E.

unfed SCOT-KO neonates administered [^{13}C]octanoate, suckling-induced hyperketonemia correlated with the emergence of a 90% decrease in ^{13}C-βOHB enrichment in milk-fed P0 SCOT-KO mice compared with littermate controls (Fig. 3*E*, *left*). Similar to the observations in the pools of βOHB in P1 SCOT-KO mice, suckling in P0 mice correlated with a marked expansion of the hepatic βOHB pool in SCOT-KO neonates and was associated with an 80% decrease in the abundance of ^{13}C-βOHB (Fig. 3*E*, *middle* and *right*). Diminished ^{13}C-βOHB enrichment from [^{13}C]octanoate occurred in livers of fed P0 SCOT-KO mice despite normal abundances of *Fabp1*, *Cpt1a*, *Acadm*, *Hmgcs2*, and *Bdh1* mRNAs and a 38% increase in HMGCS2 protein (supplemental Fig. S4). Together, these results indicate that suckling-induced hyperketonemia in SCOT-KO neonates diminishes the generation of ^{13}C-βOHB from [^{13}C]octanoate, without impairment of the upstream β-spiral or diminution of expression of the enzymatic mediators of fatty acid oxidation and ketogenesis.

To determine whether the acquired deficiency of *de novo* hepatic βOHB production in livers of SCOT-KO mice was mediated by hyperketonemia, we measured ketogenesis in livers explanted into culture from unfed and fed P0 SCOT-KO and littermate control mice, to isolate them from a hyperketonemic milieu. As expected, explants from unfed wild-type and SCOT-KO neonatal mice did not differ in ketogenic rate (Fig. 4*A*). However, in contrast to the defect in *de novo* synthesis of βOHB exhibited by fed P0 SCOT-KO mice *in vivo*, livers explanted from fed SCOT-KO mice exhibited normal ketogenic rates, despite the increased baseline ketone body abundance in these explants (Fig. 4*B*). Therefore, to test the hypothesis that the acquired ketogenic impairment in livers of SCOT-KO mice requires an environment in which ketone bodies accumulate, we determined the effects of hyperketonemia on hepatic βOHB production *in vivo* by performing intraperitoneal co-injections in fed wild-type P0 mice. Unlabeled AcAc, D-βOHB, or L-βOHB (L-βOHB is a by-product of fatty acid oxidation that is neither produced during hepatic ketogenesis nor is a substrate for BDH1 (30, 31)) were co-injected intraperitoneally with [^{13}C]octanoate into milk-fed P0 wild-type neonatal mice, and the hepatic βOHB pool sizes, fractional enrichments of hepatic ^{13}C-βOHB, and molar contents of ^{13}C-βOHB/mg tissue were quantified. Co-administered AcAc, L-βOHB, and D-βOHB each expanded the total βOHB pool significantly, although hepatic βOHB concentrations were greater in neonates co-injected with L- or D-βOHB compared with neonates co-injected with AcAc (Fig. 5*A*). Whereas fractional ^{13}C enrichments of βOHB from [^{13}C]octanoate were decreased in livers of mice co-injected with each of the three unlabeled ketone bodies, neonatal mice co-injected with L- or D-βOHB exhibited greater suppression of ^{13}C-βOHB enrichment than neonates co-injected with AcAc (Fig. 5*B*). However, only co-administered D-βOHB decreased the molar content/mg tissue of ^{13}C-βOHB in livers of wild-type mice (by 75%), whereas neither AcAc nor L-βOHB produced this effect (Fig. 5*C*). Because oxidation of D-βOHB to AcAc by BDH1 concomitantly reduces NAD^+ to NADH (9, 32, 33), these results suggest that the exogenously delivered D-βOHB diminished *de novo* βOHB production by shifting the equilibrium of the BDH1-catalyzed reaction toward AcAc formation.

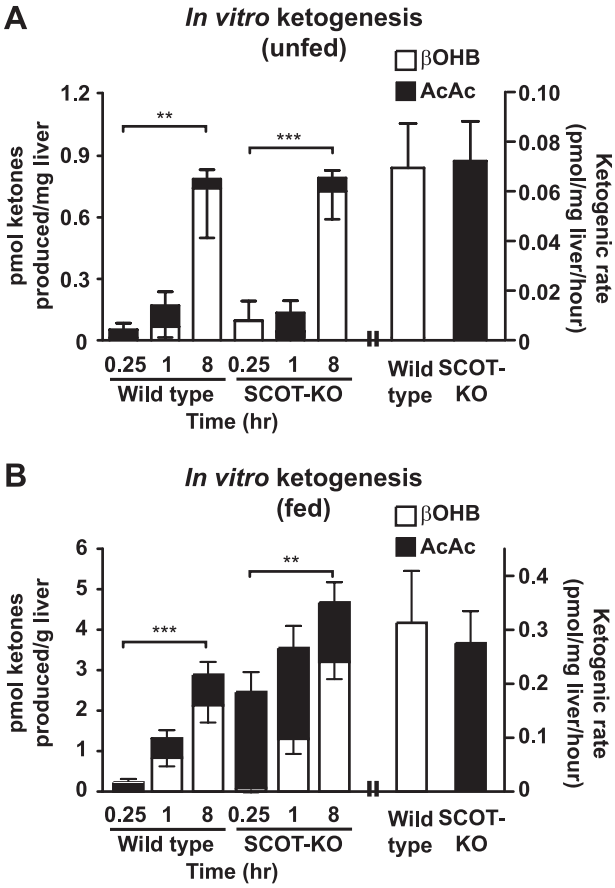

FIGURE 4. **Normal *in vitro* hepatic ketogenesis of livers from SCOT-KO mice.** Determination of ketone body production (pmol of ketone/mg of liver), 0.25, 1, and 8 h after stimulation with BSA-conjugated oleic acid (150 μM) was used to derive ketogenic rate (pmol/mg of liver per h) in liver explants derived from unfed (*A*) and fed (*B*) P0 mice. n = 4/group for unfed pups, and n = 8–10/group for fed pups. **, $p < 0.01$; ***, $p < 0.001$ by one-way ANOVA. *Error bars*, S.E.

Diminished βOHB Production by Livers of Neonatal SCOT-KO Mice Results in Oxidation of Hepatic Redox Potential—Despite the impairment of *de novo* synthesis of βOHB, livers of SCOT-KO neonates continue to channel fatty acid oxidation-derived acetyl-CoA to AcAc, which exhibits a 4-fold increase in plasma concentration between P0 and P1 in SCOT-KO mice (16). Because AcAc and D-βOHB exist in an NAD^+- and NADH-coupled equilibrium, we hypothesized that preservation of AcAc formation, but impairment of its reduction to D-βOHB would oxidize hepatic redox potential. Whereas plasma AcAc/βOHB molar ratios were elevated 3.5-fold (p = 0.03, n = 8–9/group) in fed P0 SCOT-KO mice over wild-type littermate controls, these ratios spanned a large dynamic range among SCOT-KO animals (Fig. 6*A*), and abundances of total NAD^+ and NADH were normal in both livers and skeletal muscle of fed P0 SCOT-KO mice (Fig. 6, *B* and *C*). Plasma AcAc/βOHB ratios were increased 10-fold ($p = 1.98 \times 10^{-8}$, n = 11–14/group) in P1 SCOT-KO mice compared with littermate controls, but in contrast to fed P0 SCOT-KO mice, they exhibited less variability (Fig. 6*D*). Correspondingly, livers of P1 SCOT-KO mice exhibited a 3-fold increased ratio of NAD^+/

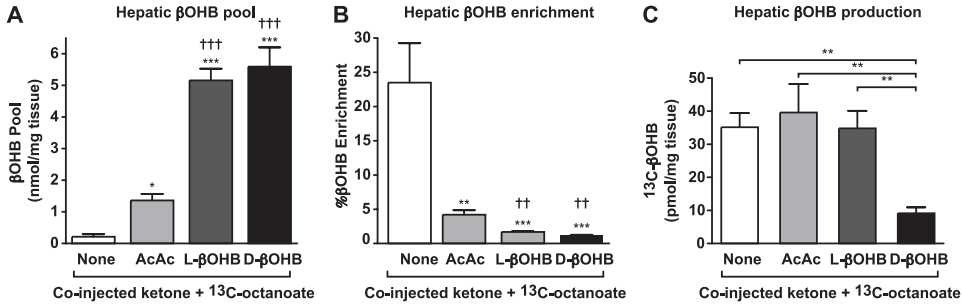

FIGURE 5. **D-βOHB inhibits neonatal hepatic ketogenesis *in vivo*.** Total βOHB pools (*A*), fractional ^{13}C enrichments of βOHB (*B*), and ^{13}C-βOHB concentrations (*C*) 20 min after intraperitoneal injection of sodium [1,2,3,4-$^{13}C_4$]octanoate (10 μmol/g of body weight) alone or co-injected with [^{13}C]octanoate plus 20 μmol/g of body weight of unlabeled AcAc, L-βOHB, or D-βOHB, in livers of milk-fed P0 mice. The [^{13}C]octanoate alone datasets (the *white bars* in these *panels*) are reproduced from Fig. 3*E* for comparison. $n = 5$–7/group for each *panel*. *, $p < 0.05$; **, $p < 0.01$; ***, $p < 0.001$ *versus* wild-type neonates injected with [^{13}C]octanoate alone, or as indicated by 1-way ANOVA. ††, $p < 0.01$; †††, $p < 0.001$ *versus* AcAc co-injected neonates. *Error bars*, S.E.

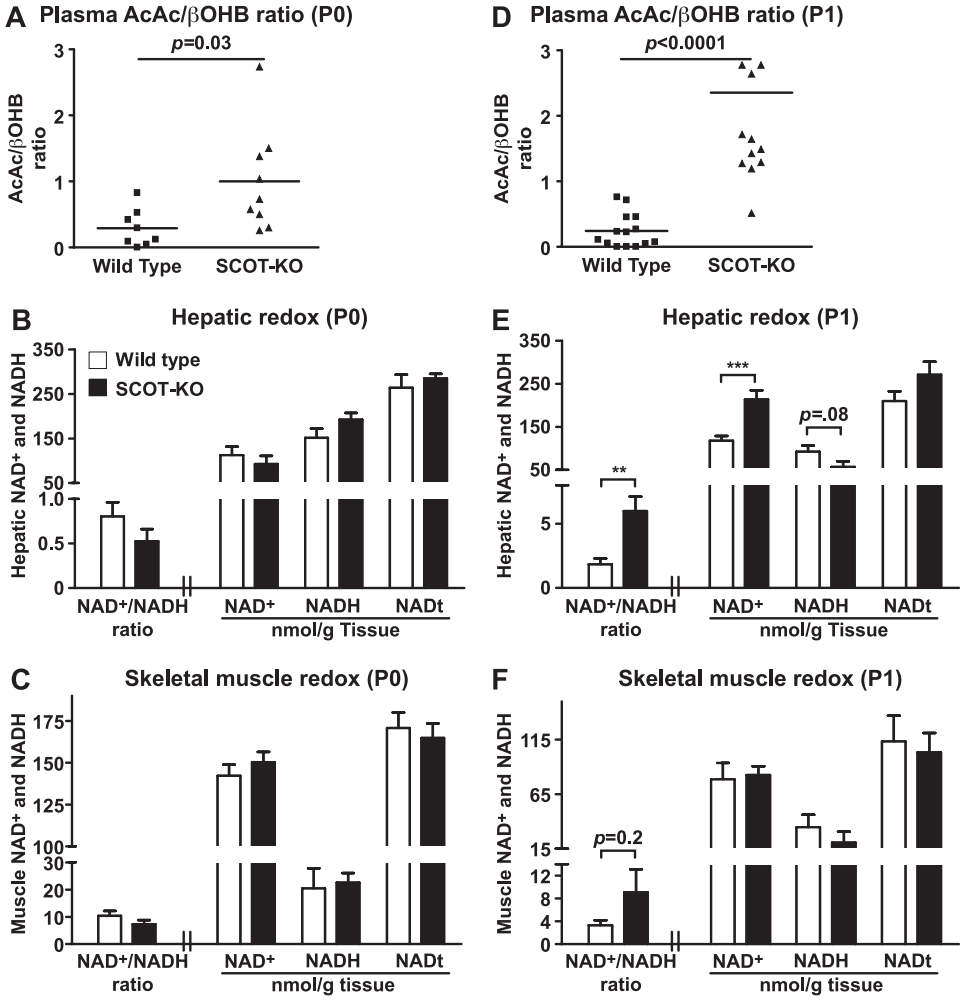

FIGURE 6. **Oxidized hepatic redox potential in P1 SCOT-KO mice.** *A*, plasma AcAc/D-βOHB molar ratios in milk-fed P0 mice. $n = 8$–9/group. *B* and *C*, NAD^+/NADH ratios, NAD^+, NADH, and total NAD (NAD^+ + NADH; NADt (nmol/g of tissue)) in livers ($n = 5$/group) (*B*) and skeletal muscles (*C*) of fed P0 neonates ($n = 6$/group). *D*, plasma AcAc/D-βOHB molar ratios in P1 mice. $n = 11$–14/group. *E* and *F*, NAD^+/NADH ratios, [NAD^+], [NADH], and [NADt] (nmol/g of tissue) in livers (*E*) and skeletal muscles (*F*) of P1 wild-type and SCOT-KO mice. $n = 13$–14/group. **, $p < 0.01$; ***, $p < 0.001$ by Student's *t* test. *Error bars*, S.E.

NADH concentrations (Fig. 6*E*). This effect was neither attributable to, nor contributed to, altered hepatic abundances of mRNAs encoding NAMPT, CD38, SIRT1, or Rictor (supplemental Fig. S5). Redox potential was unaltered in skeletal muscles of P1 SCOT-KO mice (Fig. 6*F*), consistent with the notion that persistent AcAc production by the liver is the primary driver of the redox abnormality of P1 SCOT-KO mice. Because SCOT is normally considered absent in hepatocytes (11, 17, 34), and only a scant amount of SCOT was detected in neonatal hepatic lysates (supplemental Fig. S6), these results indicate that peripheral disposal of ketone bodies is required to prevent oxidation of hepatic redox potential.

DISCUSSION

Ketone bodies provide an alternative fuel in states of diminished carbohydrate supply (1, 3, 4). Ketone body oxidation is required for adaptation to birth in mice and for adaptation to low carbohydrate states in humans (16, 35). Here we show that extrahepatic ketone body oxidation is essential for preservation of hepatic metabolic homeostasis during the ketogenic neonatal period because the absence of ketone body oxidation causes impaired hepatic terminal fatty acid oxidation, altered pyruvate metabolism, and diminished *de novo* βOHB production, which results in oxidation of hepatic redox potential.

Germline SCOT-KO neonates succumb to neonatal hypoglycemia. Increased peripheral oxidation of lactate and glucose contributes to hypolactatemia and hypoglycemia (16) and increases the gluconeogenic burden of SCOT-KO livers. These mice also develop increased blood amino acid concentrations, indicating that hypoglycemia and the inability to derive high energy phosphates from ketone bodies likely stimulate skeletal muscle proteolysis. Whereas increased blood amino acid concentrations indicate that amino acid supply exceeds hepatic utilization, a subset of these amino acids yields gluconeogenic carbon backbones within liver and replenishes TCA cycle intermediates via anaplerosis (24). Notably, blood alanine concentrations are decreased in SCOT-KO neonates, although absolute plasma pyruvate concentrations are preserved, suggesting that pyruvate generation via both the glucose-alanine and Cori cycles increases to support increased gluconeogenic demand. Because livers of SCOT-KO neonates successfully produce glucose from exogenously delivered pyruvate, impairments of the hepatic gluconeogenic machinery do not account for hypoglycemia. In fact, gluconeogenic enzymes, which normally exhibit significant postnatal inductions (1), are further induced in livers of SCOT-KO neonates. Together, these data suggest that the availability of gluconeogenic substrates (*i.e.* alanine and the lactate + pyruvate pool), and not expression of enzymatic mediators of gluconeogenesis, exacerbates the mismatch between neonatal hepatic glucose production and extrahepatic glucose requirements in mice that lack CoA transferase activity. In states of limited dietary carbohydrate supply, >60% of hepatic gluconeogenesis is derived from pyruvate (36). Upon carboxylation by pyruvate carboxylase, pyruvate supplies the TCA cycle with the intermediate oxaloacetate, which can either remain in the cycle to facilitate terminal oxidation of acetyl-CoA or efflux into the gluconeogenic pathway through PEPCK-dependent conversion to phosphoenolpyruvate (24, 37). Such "pyruvate cycling" governs rates of anaplerosis and TCA cycle intermediate efflux (37), which normally exceed the rate of TCA cycle flux in the liver (38). Although limited pyruvate pool availability precludes preservation of euglycemia, transcriptional induction of these enzymatic mediators of pyruvate cycling may initially help support gluconeogenesis in livers of SCOT-KO mice.

Hyperketonemic states, both physiological and pathophysiological, are almost always characterized by plasma AcAc/βOHB molar ratios that are <1. SCOT-KO mice present a unique hyperketonemic state in which the AcAc/βOHB molar ratio is >1. Following their first high fat, low carbohydrate milk meal, SCOT-KO mice develop hyperketonemia, which becomes associated with diminished *de novo* production of D-βOHB. NMR studies in wild type mice co-injected with the fatty acid [^{13}C]octanoate and unlabeled ketone bodies indicate that increased circulating D-βOHB in germline SCOT-KO mice diminishes hepatic production of βOHB. In the final ketogenic reaction, AcAc is reduced to D-βOHB in an NAD^+/NADH-coupled equilibrium reaction catalyzed by BDH1 that normally favors βOHB production (8–10). However, the equilibrium of the BDH1 reaction is sensitive to concentrations of both AcAc and D-βOHB, such that increases in the molar concentrations of one partner of the couple diminish the reduction/oxidation of the other (33). Because livers of SCOT-KO mice initially produce D-βOHB in a normal fashion (Figs. 3*B* and 4), a model emerges in which loss of peripheral ketone body oxidation results in pooling of D-βOHB, which causes the equilibrium of BDH1 to shift toward AcAc, such that AcAc becomes the primary ketone body synthesized by *de novo* hepatic ketogenesis. Rising AcAc concentrations initially counteract the propensity of D-βOHB to reduce hepatic redox potential, explaining why hepatic NAD^+/NADH ratios are normal in fed P0 SCOT-KO mice. Continued channeling of β-oxidation-derived acetyl-CoA to AcAc ultimately results in the high plasma AcAc/βOHB ratios, and thus elevated hepatic NAD^+/NADH ratios observed in P1 germline SCOT-KO mice.

The development of oxidized hepatic redox potential may partially explain the alteration of pyruvate and fatty acid handling in livers of P1 SCOT-KO mice. In states of high fat/low carbohydrate nutrient supply, the vast majority of pyruvate delivered to the liver enters the TCA cycle via carboxylation, rather than decarboxylation to acetyl-CoA via the PDH complex (39). Whereas the pyruvate carboxylation pathway is active, and possibly augmented in livers of P1 SCOT-KO mice, the ^{13}C fractional enrichments of glutamate observed in both (i) the [^{13}C]octanoate + unlabeled pyruvate and (ii) the [^{13}C]pyruvate experiments both suggest that flux of pyruvate through PDH is relatively increased in livers of SCOT-KO mice. Phosphorylation of the E1 α subunit of PDH was not diminished in livers of P1 SCOT-KO mice, which suggests equal PDH activity. However, pyruvate concentrations in these experiments were high enough that PDH flux could be governed by the concentrations of its cofactor, NAD^+, and one of its allosteric inhibitors, NADH, whose concentrations are increased and decreased, respectively, in livers of P1 SCOT-KO neonates (27, 29, 40). These findings are consistent with the notion that increased gluconeogenic demand and an oxidized hepatic redox potential together support a state of increased pyruvate consumption that culminates in the diminished pyruvate pools that lead to hypoglycemia in SCOT-KO mice. An additional consequence of augmented contribution of pyruvate to the TCA cycle through acetyl-CoA is diminished contribution of fatty acid oxidation-derived acetyl-CoA. Whereas the NMR studies of P1 SCOT-KO mice injected with [^{13}C]octanoate alone indicated equal fractional enrichment of [^{13}C]glutamate, this observation was obtained in the context of a diminished total glutamate pool, raising the possibility that absolute flux of fatty acids through terminal oxidation is reduced in livers of P1 SCOT-KO neonates. Increased circulating concentrations of

short chain acylcarnitines in P1 SCOT-KO mice support this hypothesis. These integrated mechanisms merit further evaluation in the pathogenesis of human neonatal hypoglycemia, a high morbidity condition with an incidence of 10% (41).

At birth, mammals experience a shift toward a lipid-dominated energy economy, inducing hepatic fatty acid oxidation, ketogenesis, and gluconeogenesis (1). Although rodents are born at an earlier developmental stage and exhibit lower neonatal body fat percentages, they suckle milk with higher fat contents than humans, and physiological ketosis develops rapidly after birth in both (1, 2, 23). Case reports indicate that HMGCS2- and SCOT-deficient humans adapt poorly to nutrient states that are marked by diminished carbohydrate intake. Human HMGCS2 deficiency results in pediatric hypoketonemic hypoglycemia (42), and human CoA transferase deficiency manifests as spontaneous pediatric ketoacidosis (43, 44), which in severe cases is associated with hypoglycemia and may account for a subset of idiopathic ketotic hyopoglycemia cases (45, 46). SCOT-KO mice die in a manner that mimics human sudden infant death syndrome (SIDS)/sudden unexpected death in infancy (SUDI), the leading cause of death of U.S. infants after the age of 1 month (47). Inborn errors of ketone body oxidation are not currently assessed on any statewide screening protocols in the United States (48). Therefore, these metabolic abnormalities merit further evaluation, as supported by a recent observational study in which metabolic autopsies performed on 255 SIDS patients detected three individuals with underlying disorders of ketone body metabolism (49). Thus, a small subset of sudden infant death cases could be attributable to undetected defects in ketone body oxidation.

Due to their small size and delicate nature, steady-state analyses of metabolic flux in neonatal mice are not currently possible. Therefore, we performed NMR substrate fate mapping after bolus injections of octanoate to quantify hepatic fatty acid fate in neonatal mice. This medium chain fatty acid avidly enters the mitochondrial matrix independently of allosterically regulated mitochondrial carnitine palmitoyltransferase 1a (4) and thus reports the activities of β-oxidation, fractional contribution to the TCA cycle, and ketogenesis.

We have demonstrated that global disruption of ketone body oxidation reprograms hepatic intermediary metabolism, initiating a cascade that alters ketogenesis and oxidizes hepatic redox potential and ultimately consumes pyruvate at the expense of terminal hepatic fatty acid oxidation, resulting in accumulation of circulating short chain acylcarnitines and hepatic triacylglycerols. Thus, extrahepatic ketone body oxidation helps integrate hepatic ketogenesis, redox potential, fatty acid oxidation, and glucose production in the neonatal period. Future studies will be needed to determine whether these relationships extend to other physiological and pathophysiological states characterized by excess fatty acid availability and limited carbohydrate supply (or inefficient carbohydrate utilization), including starvation, adherence to low carbohydrate diets, and types 1 and 2 diabetes.

Acknowledgments—We thank Shin-ichiro Imai and Rebecca Schugar for helpful discussions, Laura Kyro for assistance with graphics, and Ashley Moll and Debra Whorms for technical assistance.

REFERENCES

1. Girard, J., Ferré, P., Pégorier, J. P., and Duée, P. H. (1992) Adaptations of glucose and fatty acid metabolism during perinatal period and suckling-weaning transition. *Physiol. Rev.* **72,** 507–562
2. Ward Platt, M., and Deshpande, S. (2005) Metabolic adaptation at birth. *Semin. Fetal Neonatal Med.* **10,** 341–350
3. Robinson, A. M., and Williamson, D. H. (1980) Physiological roles of ketone bodies as substrates and signals in mammalian tissues. *Physiol. Rev.* **60,** 143–187
4. McGarry, J. D., and Foster, D. W. (1980) Regulation of hepatic fatty acid oxidation and ketone body production. *Annu. Rev. Biochem.* **49,** 395–420
5. Cotter, D. G., Schugar, R. C., and Crawford, P. A. (2013) Ketone body metabolism and cardiovascular disease. *Am. J. Physiol. Heart Circ. Physiol.* **304,** H1060–1076
6. Sunny, N. E., Satapati, S., Fu, X., He, T., Mehdibeigi, R., Spring-Robinson, C., Duarte, J., Potthoff, M. J., Browning, J. D., and Burgess, S. C. (2010) Progressive adaptation of hepatic ketogenesis in mice fed a high-fat diet. *Am. J. Physiol. Endocrinol. Metab.* **298,** E1226–1235
7. Satapati, S., Sunny, N. E., Kucejova, B., Fu, X., He, T. T., Méndez-Lucas, A., Shelton, J. M., Perales, J. C., Browning, J. D., and Burgess, S. C. (2012) Elevated TCA cycle function in the pathology of diet-induced hepatic insulin resistance and fatty liver. *J. Lipid Res.* **53,** 1080–1092
8. Hegardt, F. G. (1999) Mitochondrial 3-hydroxy-3-methylglutaryl-CoA synthase: a control enzyme in ketogenesis. *Biochem. J.* **338,** 569–582
9. Lehninger, A. L., Sudduth, H. C., and Wise, J. B. (1960) D-β-Hydroxybutyric dehydrogenase of mitochondria. *J. Biol. Chem.* **235,** 2450–2455
10. Bock, H., and Fleischer, S. (1975) Preparation of a homogeneous soluble D-β-hydroxybutyrate apodehydrogenase from mitochondria. *J. Biol. Chem.* **250,** 5774–5781
11. Williamson, D. H., Bates, M. W., Page, M. A., and Krebs, H. A. (1971) Activities of enzymes involved in acetoacetate utilization in adult mammalian tissues. *Biochem. J.* **121,** 41–47
12. Stern, J. R., Coon, M. J., Del Campillo, A., and Schneider, M. C. (1956) Enzymes of fatty acid metabolism. IV. Preparation and properties of coenzyme A transferase. *J. Biol. Chem.* **221,** 15–31
13. Bougneres, P. F., Lemmel, C., Ferré, P., and Bier, D. M. (1986) Ketone body transport in the human neonate and infant. *J. Clin. Invest.* **77,** 42–48
14. Yang, S. Y., He, X. Y., and Schulz, H. (1987) Fatty acid oxidation in rat brain is limited by the low activity of 3-ketoacyl-coenzyme A thiolase. *J. Biol. Chem.* **262,** 13027–13032
15. Cunnane, S. C., and Crawford, M. A. (2003) Survival of the fattest: fat babies were the key to evolution of the large human brain. *Comp. Biochem. Physiol. A Mol. Integr. Physiol.* **136,** 17–26
16. Cotter, D. G., d'Avignon, D. A., Wentz, A. E., Weber, M. L., and Crawford, P. A. (2011) Obligate role for ketone body oxidation in neonatal metabolic homeostasis. *J. Biol. Chem.* **286,** 6902–6910
17. Fukao, T., Song, X. Q., Mitchell, G. A., Yamaguchi, S., Sukegawa, K., Orii, T., and Kondo, N. (1997) Enzymes of ketone body utilization in human tissues: protein and messenger RNA levels of succinyl-coenzyme A (CoA): 3-ketoacid CoA transferase and mitochondrial and cytosolic acetoacetyl-CoA thiolases. *Pediatr. Res.* **42,** 498–502
18. Cotter, D. G., Schugar, R. C., Wentz, A. E., d'Avignon, D. A., and Crawford, P. A. (2013) Successful adaptation to ketosis by mice with tissue-specific deficiency of ketone body oxidation. *Am. J. Physiol. Endocrinol. Metab.* **304,** E363–374
19. Wentz, A. E., d'Avignon, D. A., Weber, M. L., Cotter, D. G., Doherty, J. M., Kerns, R., Nagarajan, R., Reddy, N., Sambandam, N., and Crawford, P. A. (2010) Adaptation of myocardial substrate metabolism to a ketogenic nutrient environment. *J. Biol. Chem.* **285,** 24447–24456
20. Crawford, P. A., Crowley, J. R., Sambandam, N., Muegge, B. D., Costello, E. K., Hamady, M., Knight, R., and Gordon, J. I. (2009) Regulation of myocardial ketone body metabolism by the gut microbiota during nutrient deprivation. *Proc. Natl. Acad. Sci. U.S.A.* **106,** 11276–11281
21. Jones, J. G., Hansen, J., Sherry, A. D., Malloy, C. R., and Victor, R. G. (1997) Determination of acetyl-CoA enrichment in rat heart and skeletal muscle by 1H nuclear magnetic resonance analysis of glutamate in tissue extracts. *Anal. Biochem.* **249,** 201–206

22. Dietzen, D. J., Weindel, A. L., Carayannopoulos, M. O., Landt, M., Normansell, E. T., Reimschisel, T. E., and Smith, C. H. (2008) Rapid comprehensive amino acid analysis by liquid chromatography/tandem mass spectrometry: comparison to cation exchange with post-column ninhydrin detection. *Rapid Commun. Mass Spectrom.* **22,** 3481–3488
23. Cahill, G. F., Jr. (2006) Fuel metabolism in starvation. *Annu. Rev. Nutr.* **26,** 1–22
24. Owen, O. E., Kalhan, S. C., and Hanson, R. W. (2002) The key role of anaplerosis and cataplerosis for citric acid cycle function. *J. Biol. Chem.* **277,** 30409–30412
25. Ziegler, A., Zaugg, C. E., Buser, P. T., Seelig, J., and Künnecke, B. (2002) Non-invasive measurements of myocardial carbon metabolism using ^{13}C NMR spectroscopy. *NMR Biomed.* **15,** 222–234
26. Andrews, M. T., Russeth, K. P., Drewes, L. R., and Henry, P. G. (2009) Adaptive mechanisms regulate preferred utilization of ketones in the heart and brain of a hibernating mammal during arousal from torpor. *Am. J. Physiol. Regul. Integr. Comp. Physiol.* **296,** R383–393
27. Hue, L., and Taegtmeyer, H. (2009) The Randle cycle revisited: a new head for an old hat. *Am. J. Physiol. Endocrinol. Metab.* **297,** E578–591
28. Holness, M. J., and Sugden, M. C. (2003) Regulation of pyruvate dehydrogenase complex activity by reversible phosphorylation. *Biochem. Soc. Trans.* **31,** 1143–1151
29. Taylor, S. I., Mukherjee, C., and Jungas, R. L. (1975) Regulation of pyruvate dehydrogenase in isolated rat liver mitochondria: effects of octanoate, oxidation-reduction state, and adenosine triphosphate to adenosine diphosphate ratio. *J. Biol. Chem.* **250,** 2028–2035
30. Scofield, R. F., Brady, P. S., Schumann, W. C., Kumaran, K., Ohgaku, S., Margolis, J. M., and Landau, B. R. (1982) On the lack of formation of L-(+)-3-hydroxybutyrate by liver. *Arch. Biochem. Biophys.* **214,** 268–272
31. Lincoln, B. C., Des Rosiers, C., and Brunengraber, H. (1987) Metabolism of *S*-3-hydroxybutyrate in the perfused rat liver. *Arch. Biochem. Biophys.* **259,** 149–156
32. Williamson, D. H., Lund, P., and Krebs, H. A. (1967) The redox state of free nicotinamide-adenine dinucleotide in the cytoplasm and mitochondria of rat liver. *Biochem. J.* **103,** 514–527
33. Preuveneers, M. J., Peacock, D., Crook, E. M., Clark, J. B., and Brocklehurst, K. (1973) D-3-Hydroxybutyrate dehydrogenase from *Rhodopseudomonas spheroides*: kinetics of radioisotope redistribution at chemical equilibrium catalysed by the enzyme in solutions. *Biochem. J.* **133,** 159–164
34. Orii, K. E., Fukao, T., Song, X. Q., Mitchell, G. A., and Kondo, N. (2008) Liver-specific silencing of the human gene encoding succinyl-CoA:3-ketoacid CoA transferase. *Tohoku J. Exp. Med.* **215,** 227–236
35. Niezen-Koning, K. E., Wanders, R. J., Ruiter, J. P., Ijlst, L., Visser, G., Reitsma-Bierens, W. C., Heymans, H. S., Reijngoud, D. J., and Smit, G. P. (1997) Succinyl-CoA:acetoacetate transferase deficiency: identification of a new patient with a neonatal onset and review of the literature. *Eur. J. Pediatr.* **156,** 870–873
36. Burgess, S. C., Leone, T. C., Wende, A. R., Croce, M. A., Chen, Z., Sherry, A. D., Malloy, C. R., and Finck, B. N. (2006) Diminished hepatic gluconeogenesis via defects in tricarboxylic acid cycle flux in peroxisome proliferator-activated receptor γ co-activator-1α (PGC-1α)-deficient mice. *J. Biol. Chem.* **281,** 19000–19008
37. Burgess, S. C., Hausler, N., Merritt, M., Jeffrey, F. M., Storey, C., Milde, A., Koshy, S., Lindner, J., Magnuson, M. A., Malloy, C. R., and Sherry, A. D. (2004) Impaired tricarboxylic acid cycle activity in mouse livers lacking cytosolic phosphoenolpyruvate carboxykinase. *J. Biol. Chem.* **279,** 48941–48949
38. Magnusson, I., Schumann, W. C., Bartsch, G. E., Chandramouli, V., Kumaran, K., Wahren, J., and Landau, B. R. (1991) Noninvasive tracing of Krebs cycle metabolism in liver. *J. Biol. Chem.* **266,** 6975–6984
39. Merritt, M. E., Harrison, C., Sherry, A. D., Malloy, C. R., and Burgess, S. C. (2011) Flux through hepatic pyruvate carboxylase and phosphoenolpyruvate carboxykinase detected by hyperpolarized ^{13}C magnetic resonance. *Proc. Natl. Acad. Sci. U.S.A.* **108,** 19084–19089
40. Batenburg, J. J., and Olson, M. S. (1976) Regulation of pyruvate dehydrogenase by fatty acid in isolated rat liver mitochondria. *J. Biol. Chem.* **251,** 1364–1370
41. Harris, D. L., Weston, P. J., and Harding, J. E. (2012) Incidence of neonatal hypoglycemia in babies identified as at risk. *J. Pediatr.* **161,** 787–791
42. Aledo, R., Zschocke, J., Pié, J., Mir, C., Fiesel, S., Mayatepek, E., Hoffmann, G. F., Casals, N., and Hegardt, F. G. (2001) Genetic basis of mitochondrial HMG-CoA synthase deficiency. *Hum. Genet.* **109,** 19–23
43. Tildon, J. T., and Cornblath, M. (1972) Succinyl-CoA: 3-ketoacid CoA-transferase deficiency: a cause for ketoacidosis in infancy. *J. Clin. Invest.* **51,** 493–498
44. Kassovska-Bratinova, S., Fukao, T., Song, X. Q., Duncan, A. M., Chen, H. S., Robert, M. F., Pérez-Cerdá, C., Ugarte, M., Chartrand, C., Vobecky, S., Kondo, N., and Mitchell, G. A. (1996) Succinyl CoA:3-oxoacid CoA transferase (SCOT): human cDNA cloning, human chromosomal mapping to 5p13, and mutation detection in a SCOT-deficient patient. *Am. J. Hum. Genet.* **59,** 519–528
45. Berry, G. T., Fukao, T., Mitchell, G. A., Mazur, A., Ciafre, M., Gibson, J., Kondo, N., and Palmieri, M. J. (2001) Neonatal hypoglycaemia in severe succinyl-CoA:3-oxoacid CoA-transferase deficiency. *J. Inher. Metab. Dis.* **24,** 587–595
46. Huidekoper, H. H., Duran, M., Turkenburg, M., Ackermans, M. T., Sauerwein, H. P., and Wijburg, F. A. (2008) Fasting adaptation in idiopathic ketotic hypoglycemia: a mismatch between glucose production and demand. *Eur. J. Pediatr.* **167,** 859–865
47. Miniño, A. M., Xu, J., and Kochanek, K. D. (2010) *National Vital Statistics Rep. CDC Control Prevention* **59,** 1–52
48. Mitchell, G. A., and Fukao, T. (2000) in *The Online Metabolic and Molecular Bases of Inherited Diseases* (*OMMBID*) (Beaudet, A., Vogelstein, B., Kinzler, K. W., Antonarakis, S., and Ballabio, A., eds) p. 12, The McGraw-Hill Companies, Columbus, OH
49. Pryce, J. W., Weber, M. A., Heales, S., Malone, M., and Sebire, N. J. (2011) Tandem mass spectrometry findings at autopsy for detection of metabolic disease in infant deaths: postmortem changes and confounding factors. *J. Clin. Pathol.* **64,** 1005–1009